Detailed investigation of energy transfers in homogeneous stratified turbulence*

F. S. Godeferd and C. Cambon

Citation: Physics of Fluids **6**, 2084 (1994); doi: 10.1063/1.868214
View online: http://dx.doi.org/10.1063/1.868214
View Table of Contents: http://scitation.aip.org/content/aip/journal/pof2/6/6?ver=pdfcov
Published by the AIP Publishing

Detailed investigation of energy transfers in homogeneous stratified turbulence*

F. S. Godeferd and C. Cambon
Laboratoire de Mécanique des Fluides et d'Acoustique, URA CNRS n° 263, Ecole Centrale de Lyon, 69131 Ecully Cedex, France

(Received 23 March 1993; accepted 23 February 1994)

This paper investigates some irreversible mechanisms occurring in homogeneous stably stratified turbulent flows. In terms of the eigenmodes of the linear regime, the velocity-temperature field is decomposed into a vortex and two wavy components. Using an eddy-damped quasinormal Markovian (EDQNM) closure with the axisymmetry hypothesis, an analysis of the anisotropic energy transfers between the vortex kinetic energy, the wave kinetic and potential energy is made. Within the light of triadic exchanges, and by analogy of the resonance condition for three linearly interacting gravity waves, the closure model allows one to compute the detailed transfers for eight types of interactions. Results of the calculations include time evolution plots, for the isotropic closure model as well as two different types of the anisotropic closure. The pure vortical interactions are shown to be responsible for the irreversible anisotropic structure created by stable stratification, and this structure prevents the inverse cascade of two-dimensional turbulence.

I. INTRODUCTION

There is extensive literature available on different aspects—statistical, structural, or dynamical—of turbulent flows subjected to buoyancy forces in a stably stratified (in density or temperature) field (see Hopfinger[1] for a review of experimental and numerical studies).

The severe restriction of vertical (i.e., along the mean density gradient) motion is the most important characteristic of these flows. In addition, it is suggested that the flow is organized in thin layers with a strong vertical variability, so that the velocity field is almost "two-component" but very far from being "two-dimensional."

The latter caveat is of prime importance to avoid confusion with almost two-dimensional flows created in certain conditions by solid body rotation or an external magnetic field (see Cambon and Godeferd[2] and Reynolds,[3] who distinguished "componentality" and "dimensionality"). Accordingly, quasi two-dimensional will only refer to a flow in which the variability of fluctuating quantities is severely restricted in one direction (chosen as the vertical), or $\partial/\partial x_\parallel \to 0$; such a flow is rather organized in columnar structures, but vertical motion ($u_\parallel$) is not necessarily excluded. On the other hand, quasi two-component will refer to a flow where a component of the fluctuating velocity field is small ($u_\parallel \to 0$) with a possible strong variability $\partial/\partial x_\parallel$ of the other components or flow characteristics. Such a flow is rather organized in a piling up of horizontal pancakes weakly correlated with one another. From a statistical point of view, quasi two-dimensional and quasi two-component flows can be described (and discriminated) using both single-point velocity correlations and integral length scales in several directions. Of course, a fully anisotropic two-point statistical description is relevant, as discussed in the following.

The problem in which we are interested also involves a dynamical point of view: which mechanisms are responsible for the transition from a three-dimensional homogeneous and isotropic turbulence towards a quasi two-component state (highly anisotropic)? More generally and concisely, why, how, and when does homogeneous turbulence subjected to stratification become two-component? Some heuristic arguments[4] amounted to a limitation (decreasing value with decreasing Froude number) of $\langle u_\parallel^2 \rangle$ or the integral length scales with vertical separation ($L_\parallel$), but the problem of transition is avoided. In the same way, the linearized equations (in the limit of zero Froude number) yield the collapse of vertical motion *if the time derivative is dropped out.* The latter argument is analogous to the Taylor–Proudman theorem used to justify the two-dimensional structure of turbulence subjected to strong rotation. Although they suggest what the final stage of transition is, such arguments cannot explain the dynamics of this transition in the absence of a slow external time scale (other than the Brünt–Väisälä frequency and the turbulent turnover time) and in the absence of nonlinear interactions *explicitly* investigated.

Looking at the detailed equations for double and triple correlations (at two points), it is clear that the linear regime reflected by double correlations dynamics in the absence of triple correlations [according to the so-called (improperly) Rapid Distortion Theory by Hunt, Stretch, and Britter,[5] see also vanHaren[6]] cannot create the transition. In the linear limit, a periodic exchange between a part of the kinetic energy and the potential energy (linked to the temperature variance) is observed, but no important irreversible anisotropy is created. On the other hand, DNS and two-point closures (quoted below) have given the evidence that an irreversible anisotropic trend, consistent with the first phase of a transition towards a quasi two-component state, is induced by spectral transfer terms connected with triple correlations, for sufficiently low Froude number (but not too small) and sufficiently high Reynolds numbers, indicating the essential role of nonlinear interactions in the transition process.

In this paper, detailed transfer terms are closed using a

*Originally presented at the Special Symposium in honor of William C. Reynolds 60th birthday, 22–23 March 1993.

 1070-6631/94/6(6)/2084/17/$6.00

generalized EDQNM theory (Eddy Damped Quasinormal Markovian) theory. A particular emphasis is given to the analytical treatment of linear operators in the equations for the fluctuating quantities (velocity, temperature) and their statistical correlations up to third order, whereas the closure method [7] itself will be briefly recalled.

Velocity and temperature fields are decomposed in terms of the eigenmodes of the linear regime equations, in order to diagonalize the linear operator and to identify their nonlinear interactions in the transfer terms. From a physical point of view, the linear regime consists of both vortical contributions unaffected by the stratification and internal gravity waves,[8] generated by some perturbation. In this respect, stably stratified homogeneous turbulence can be regarded as the superposition, in a nonlinear regime, of infinitely many internal waves propagating in all directions, generated by excitations continuously distributed over the whole domain.

The most sophisticated version of the model,[9] called EDQNM2 is based upon the same assumptions as the stochastic model for nonlinear Rossby waves used by Holloway and Hendershot,[10] but its derivation involves more complicated algebra because the model for Rossby waves is quasi two-dimensional (β-plane approximation). Our model was also successfully applied to rotating turbulence;[11] it gave guidelines for subsequent theoretical, computational, and experimental works.[12,13] These studies have brought a crucial contribution to the problem: why, how, and when does homogeneous turbulence become two-dimensional under solid body rotation through nonlinear effects.

Going back to the problem of stably stratified turbulence, EDQNM was used by Carnevale and Frederiksen[14] but their effort was limited by a planar geometry. Our objective, when using a specific EDQNM model, is twofold:

(i) Capture all the anisotropic features of the homogeneous flow by computing a complete spectral tensor of double correlations (velocity and temperature), including angular dependence in spectral space.

(ii) Among the detailed interactions involved in the energy transfer spectra, identify the most efficient. This selection is a prerequisite for building simpler models, directly applicable to complex geophysical or engineering flows (see for example Uittenbogaard and Baron[15]).

In the simplest configuration consistent with axisymmetry (around the vertical axis which bears the gravity and the mean temperature gradient), the spectral tensor is generated by four spectra, each of which depends on both the wave number k and its angle θ_k to the vertical direction. In accordance with Riley *et al.*[8] and Cambon,[16] Φ_1, Φ_2, and Φ_3 are vortex, kinetic wave, and potential energy spectra, whereas the fourth, Ψ, generates the buoyancy flux.

The directional dependence (θ_k) is a key characteristic for discriminating quasi two-dimensional and quasi two-component flows: in the first case, the spectral density of energy tends to be concentrated on horizontal wave vectors (2-D domain) whereas it is concentrated on vertical wave vectors (1-D domain) in the second case (see Fig. 1). The conical structure of the spectral region that contains energy

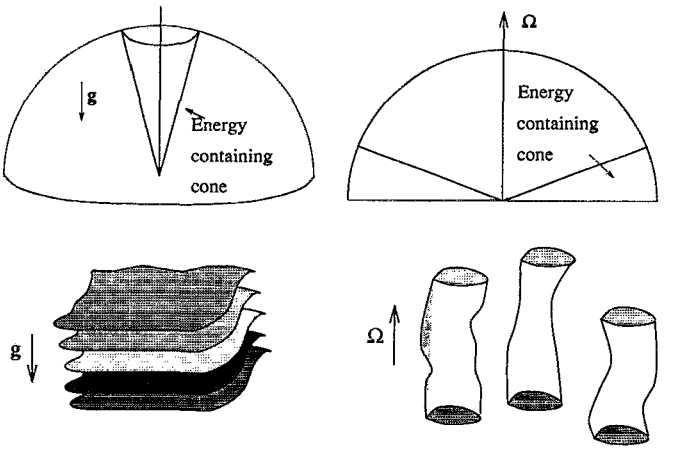

FIG. 1. Representation of the spectral angular dependence occurring in stratified (top left) and rotating (top right) turbulence, with the corresponding schematic physical structures: layered flow (bottom left) for stratification; columnar vertically correlated shapes (bottom right) for rotation.

can be quantified in physical space by Moreau angles,[17] as in MHD flows, or more generally by the structure dimensionality tensor used by Reynolds[3] (see also Cambon *et al.*[18] and Cambon and Godeferd[2]).

We are also interested in quantifying the impact of corresponding energy transfer spectra at significantly high Reynolds numbers unreachable by current DNS. Direct numerical simulations take into account the complete interactions, but the statistical data processing is cumbersome as soon as one tries to split the velocity field into wave and vortex modes. In this case, the shell-averaged method used to compute energy transfer spectra leads to highly tormented curves, and anyway to solely isotropically accumulated spectra (see the results by Metais and Herring[19]).

A last interesting aspect of our EDQNM model (or the one by Holloway and Hendershot) is the link with weakly nonlinear analyses. As also stressed by Herring,[20] the turbulence effects are equivalent to a (Lorentz) broadening of the resonance condition of weak turbulence theory. This is also illustrated in fully 3-D rotating turbulence, since the concentration of spectral energy in the horizontal wave plane induced by anisotropic transfers (a nonlinear Proudman tendency, which is one of the most important results of EDQNM2[11]), has been recently recovered by Waleffe[21] using only resonance conditions.

Müller *et al.*[22] have reviewed a few weakly nonlinear techniques, and have shown that their main drawback is to neglect the interactions of the internal wave field with the vortical mode of motion. Lelong and Riley,[23] in their weakly nonlinear analysis, have identified possible resonant mechanisms between wave and vortex modes in a triadic interaction, and found some possible energy exchanges; other studies by Holloway[24] and Carnevale and Martin[25] focused on the characteristic time of triple correlations modified by the wave frequencies. Regarding recent DNS results by Ramsden and Holloway[26] on detailed wave–vortex interactions discussed further, we are able to compute such interactions here, and give statistical results by summation over a whole angular-dependent spectral transfer tensor.

Our paper is organized as follows: background equations are given in Sec. II, including a very brief derivation of EDQNM. The linear regime and the decomposition of nonlinear terms in terms of its eigenmodes are presented in Sec. III. Numerical results are shown in Secs. IV and V. Finally, a particular emphasis on physical interpretation is given in Sec. VI that is devoted to the conclusion.

II. EQUATIONS

Stably stratified homogeneous turbulence follows the Boussinesq equations:

$$\left[\frac{\partial}{\partial t}+u_j\frac{\partial}{\partial x_j}-\nu\nabla^2\right]u_i(\mathbf{x},t)+\frac{\partial}{\partial x_i}p(\mathbf{x},t)+g_i\beta\tau(\mathbf{x},t)=0,$$
$$\left[\frac{\partial}{\partial t}+u_j\frac{\partial}{\partial x_j}-\nu P_r^{-1}\nabla^2\right]\tau(\mathbf{x},t)+\gamma_i u_i(\mathbf{x},t)=0, \qquad (1)$$
$$\frac{\partial u_i}{\partial x_i}(\mathbf{x},t)=0$$

for a velocity field $\mathbf{u}(\mathbf{x},t)$ with pressure $p(\mathbf{x},t)$, and a temperature field $\tau(\mathbf{x},t)$. β is the thermometric expansivity, ν the kinematic viscosity, Pr the Prandtl number (which will be further assumed to be equal to 1). The stratification appears in the equation for τ through γ, the mean potential temperature gradient. The vector $\mathbf{g}$ is the gravity.

In spectral space, all variables are Fourier transformed as follows:

$$\hat{u}_i(\mathbf{k},t)=\frac{1}{(2\pi)^3}\int u_i(\mathbf{x},t)e^{-I\mathbf{k}\cdot\mathbf{x}}\,d^3\mathbf{x} \qquad (2)$$

with $I^2=-1$; therefore:

$$\left[\frac{\partial}{\partial t}+\nu k^2\right]\hat{u}_i(\mathbf{k},t)-P_{i3}(\mathbf{k},t)g\beta\hat{\tau}(\mathbf{k},t)$$
$$=-Ik_lP_{in}(\mathbf{k})\widehat{\langle u_l u_n\rangle}(\mathbf{k},t),$$
$$\left[\frac{\partial}{\partial t}+\nu k^2\right]\hat{\tau}(\mathbf{k},t)-\gamma\hat{u}_3(\mathbf{k},t)=-Ik_l\widehat{\langle u_l\tau\rangle}(\mathbf{k},t), \qquad (3)$$
$$P_{ij}(\mathbf{k})=\delta_{ij}-\frac{k_ik_j}{k^2}$$

so that the fluctuating pressure is removed from consideration and the solenoidal (divergence free) property of the velocity amounts to $\mathbf{k}\cdot\hat{\mathbf{u}}=0$.

We define the $\hat{\mathbf{v}}$ variable as:

$$\hat{v}_i(\mathbf{k},t)=\hat{u}_i(\mathbf{k},t)+I\frac{k_i}{k}\frac{\beta g}{N}\hat{\tau}(\mathbf{k},t)=\hat{u}_i(\mathbf{k},t)+\hat{\varphi}_i^3(\mathbf{k},t) \qquad (4)$$

which will prove very useful in order to simplify the derivation of the following equations, since it gathers both the velocity and the temperature fields. For mathematical convenience, the scalar temperature field is considered as a third *vector* mode $\hat{\varphi}_i^3$, chosen to be parallel to the wave vector since the actual velocity field $\hat{u}_i$ is orthogonal to this wave vector. Because of the orthonormal properties and the scaling coefficient $\beta g/N$, $\frac{1}{2}\hat{v}_i^*\hat{v}_i=\frac{1}{2}\hat{u}_i^*\hat{u}_i+\frac{1}{2}(\beta g/N)^2\hat{\tau}^*\hat{\tau}$ simply gives the spectral density of total energy (kinetic + potential). $N=\sqrt{\beta\gamma g}$ is the Brünt–Väisälä frequency, and I is included in the temperature mode $[\varphi^3=(\beta g/N)\tau]$ to ensure that $\mathbf{v}$ (inverse Fourier transform of $\hat{\mathbf{v}}$) is real. Further diagonalization, or expression of the components of $\hat{\mathbf{v}}$ in terms of linear combinations of the linear operator eigenmodes (see Sec. III), can be considered as a change of frame of reference as for a true 3-D vector. Hence, without loss of generality, the initial five component problem $(\hat{u}_1,\hat{u}_2,\hat{u}_3,\hat{p},\hat{\tau})$ is reduced to a three component one $(\hat{v}_1,\hat{v}_2,\hat{v}_3)$.

The evolution equation for $\hat{\mathbf{v}}$ comes from (3):

$$\left[\frac{\partial}{\partial t}+\nu k^2\right]\hat{v}_i(\mathbf{k},t)+L_{ij}(\mathbf{k})\hat{v}_j(\mathbf{k},t)$$
$$=\int_{k+p+q=0}M_{ipq}(\mathbf{k},\mathbf{p},\mathbf{q})\hat{v}_p(\mathbf{p},t)\hat{v}_q(\mathbf{q},t)\,d\mathbf{p} \qquad (5)$$

where the expressions for the linear and nonlinear operators are as follows:

$$L_{ij}(\mathbf{k})=IN\left[P_{i3}(\mathbf{k})\frac{k_j}{k}+P_{j3}(\mathbf{k})\frac{k_i}{k}\right], \qquad (6)$$
$$M_{ipq}(\mathbf{k},\mathbf{p},\mathbf{q})=-Ik_lP_{lp}(\mathbf{p})\left[P_{in}(\mathbf{k})P_{nq}(\mathbf{q})+\frac{k_iq_q}{kq}\right].$$

The spectra for second and third order correlations are:

$$\langle\hat{v}_i(\mathbf{p},t)\hat{v}_j(\mathbf{k},t)\rangle=\hat{V}_{ij}(\mathbf{k},t)\,\delta(\mathbf{k}+\mathbf{p}),$$
$$\langle\hat{v}_i(\mathbf{k},t)\hat{v}_j(\mathbf{p},t)\hat{v}_l(\mathbf{q},t)\rangle=\hat{V}_{ijl}(\mathbf{k},\mathbf{p},t)\,\delta(\mathbf{k}+\mathbf{p}+\mathbf{q}). \qquad (7)$$

These spectral tensors are governed by equations readily derived from (5):

$$\left[\frac{\partial}{\partial t}+2\nu k^2\right]\hat{V}_{ij}(\mathbf{k},t)+L_{iu}\hat{V}_{uj}+L_{jv}\hat{V}_{iv}=T_{ij}(\mathbf{k},t)+T_{ji}^*(\mathbf{k},t), \qquad (8)$$

$$\left[\frac{\partial}{\partial t}+\nu(k^2+p^2+q^2)\right]\hat{V}_{jpq}(\mathbf{k},\mathbf{p},t)$$
$$+L_{ju}\hat{V}_{upq}+L_{pv}\hat{V}_{jvq}+L_{qw}\hat{V}_{jpw}=\Omega_{jpq}(\mathbf{k},\mathbf{p},t) \qquad (9)$$

where T_{ij} accounts for the contribution of triple correlations in the dynamics of double correlations and can be exactly expressed in terms of $\hat{V}_{jpq}$, whereas Ω_{jpq} accounts for contributions of fourth order correlations (* stands for complex conjugate). In both equations, which are of the same kind as that discussed by Craya[27] in the presence of mean velocity gradients, the right-hand sides take the nonlinearity into account.

The EDQNM hypothesis applied to Eq. (5) amounts to a closure model for the right-hand side of Eq. (9), so that:

$$\left[\frac{\partial}{\partial t}+\nu(k^2+p^2+q^2)\right]\hat{V}_{jpq}(\mathbf{k},\mathbf{p},t)+L_{ju}(\mathbf{k})\hat{V}_{upq}(\mathbf{k},\mathbf{p},t)$$
$$+L_{pv}(\mathbf{p})\hat{V}_{jvq}(\mathbf{k},\mathbf{p},t)+L_{qw}(\mathbf{q})\hat{V}_{jpw}(\mathbf{k},\mathbf{p},t)$$
$$=\Omega_{jpq}^{QN}(\mathbf{k},\mathbf{p},t)-(\eta'(\mathbf{k},t)+\eta'(\mathbf{p},t)$$
$$+\eta(\mathbf{q},t))\hat{V}_{jpq}(\mathbf{k},\mathbf{p},t) \qquad (10)$$

TABLE I. Components of the velocity-temperature field and of the covariance matrix in the three relevant frames of reference. The system of linearized equations is diagonal *only* in the third frame.

	Fixed frame of reference	Craya–Herring frame $\hat{v}_i=\hat{\varphi}^j e_i^j$	Eigenframe $\hat{v}_i=\Sigma_{\varepsilon=0,\pm1}\xi_\varepsilon N_i^\varepsilon$
Vector fluctuating field $\hat{\mathbf{v}}$	$\hat{v}_1$	$\hat{\varphi}^1$	$\xi_0=\hat{\varphi}^1$ "axial vortex"
	$\hat{v}_2$	$\hat{\varphi}^2$	$\xi_{+1}=\hat{\varphi}^2+I\hat{\varphi}^3$ "wavy"
	$\hat{v}_3$	$\hat{\varphi}^3$	$\xi_{-1}=\hat{\varphi}^2-I\hat{\varphi}^3$ "wavy"
Covariance matrix $\langle\hat{\mathbf{v}}^*\otimes\hat{\mathbf{v}}\rangle$	$\langle\hat{v}_i^*\hat{v}_j\rangle\to\hat{V}_{ij}$	$\frac{1}{2}\langle\hat{\varphi}^{1*}\varphi^1\rangle\to\Phi^1$	$\frac{1}{2}\langle\xi_0^*\xi_0\rangle\to\Phi^1$
		$\frac{1}{2}\langle\hat{\varphi}^{2*}\varphi^2\rangle\to\Phi^2$	$\frac{1}{2}\langle\xi_{+1}^*\xi_{+1}\rangle\to\Phi^2+\Phi^3+\Im(\Psi)$
		$\frac{1}{2}\langle\hat{\varphi}^{3*}\varphi^3\rangle\to\Phi^3$	$\frac{1}{2}\langle\xi_{-1}^*\xi_{-1}\rangle\to\Phi^2+\Phi^3-\Im(\Psi)$
		$\frac{1}{2}\langle\hat{\varphi}^{3*}\varphi^2\rangle\to\Psi$	$\frac{1}{2}\langle\xi_{+1}^*\xi_{-1}\rangle\to\Phi^2-\Phi^3+I\Re(\Psi)$

where the right-hand side accounts for the fourth order correlations: the first term in the right-hand side, $\mathbf{\Omega}^{QN}$, is exactly expressed as for a normal law in terms of the second order correlations, and the second term in the right-hand side represents the damping effect attributed to fourth order cumulants (Orszag[7]). The detailed expression of Ω_{jpq}^{QN} in terms of $\hat{V}_{ij}$ is the same as the classical quasinormal expansion, that concerns velocity components only. Following previous works,[11] the damping term η is chosen according to standard procedures as well:[28]

$$\eta(k,t)=\nu k^2+\eta'(k,t)=\nu k^2+A\left[\int_0^k p^2E(p,t)dp\right] \quad (11)$$

where $A=0.366$ and E is the isotropically accumulated kinetic energy spectrum. The use of a single constant (A), calculated once and for all in the unstratified case, includes an implicit assumption of a "turbulent" Prandtl number close to unity.

In accordance with the model called EDQNM2,[9,11] a general solution of Eq. (10) can be found under the following form:

$$\begin{aligned}\hat{V}_{jpq}(\mathbf{k},\mathbf{p},t)=&\int_{t_0}^t G_{jl}^{ED}(\mathbf{k},t,t')M_{luv}(\mathbf{k},-\mathbf{p},-\mathbf{q})\\&\cdot G_{pm}^{ED}(\mathbf{p},t,t')\hat{V}_{um}(\mathbf{p},t)\\&\cdot G_{qn}^{ED}(\mathbf{q},t,t')\hat{V}_{vn}(\mathbf{q},t)dt'\\&+\text{other terms obtained by permuting }\mathbf{k},\mathbf{p},\mathbf{q}.\end{aligned} \quad (12)$$

Slightly different forms including the initial value of $\hat{V}_{jpq}$ (at t_0) can be used, as well as different versions of the Markovian assumption, which roughly amounts to replacing the "past" value (at time t') by the instantaneous value (at time t) of the double correlations [through $\mathbf{\Omega}^{QN}$ in Eq. (10)] in the exact solution of Eq. (10). The reader is referred to vanHaren[6] for a complete discussion.

The same closure relations could be derived using other statistical theories (DIA, TFM, RNG, etc...), and it is only the evaluation of the "renormalized" response tensor G^{ED} which distinguishes these different approaches.

In the EDQNM2 model, which most accurately corresponds to Eq. (10), G^{ED} is given by the product of the purely linear response tensor G (associated to the operator L such that $\dot{\mathsf{G}}=\mathsf{LG}$) and the viscous plus eddy damping term [associated to η in Eqs. (10) and (11)], or:

$$\mathsf{G}^{ED}(\mathbf{k},t,t')=\mathsf{G}(\mathbf{k},t-t')\ e^{-\int_{t'}^t \eta(k,t)dt''} \quad (13)$$

Neglecting η' in Eq. (10) leads to a pure quasinormal Markovian model, whereas the so-called EDQNM1 version amounts to neglecting L in Eq. (10) [or to take $G_{ij}=\delta_{ij}$ in (13)] but not in Eq. (8). In any case, a tractable form of G is derived in the following section.

III. DECOMPOSITION IN TERMS OF EIGENMODES

Although all the relevant equations were previously given (or at least summarized) in a fixed frame of reference, subsequent treatment and interpretation of results is facilitated by using two other orthonormal frames of reference quoted below: the Craya–Herring frame,[27,29] from which is readily derived an orthonormal eigenframe associated with the linear regime. This linear regime for stably stratified or rotating turbulence is considered as classic but emphasis is often given, in the literature, to some aspects (dispersion laws of the linear wave regime) without a complete definition of a basis of eigenmodes. For example, the separation into vortical mode and inertio-gravity waves is well known in the field of geostrophic turbulence, but the true two-dimensional mode (unaffected by rotation in absence of stratification) is often confused with the horizontal vortex mode (unaffected by stable stratification in absence of rotation).

Hence, we prefer to give the complete definition of the eigenmodes in this paper, in spite of a possible overlapping with the classical literature for geophysical flows. In addition, the systematic use of orthonormal frames (and a unique vector for velocity and temperature) is perhaps an original aspect: all tensorial properties are preserved by our procedure, including the definition of invariants (energy-type) and realizability constraints. Table I sums up the detail of the decomposition of the velocity-temperature vector $\hat{\mathbf{v}}$ and its covariance matrix in the three different frames of reference.

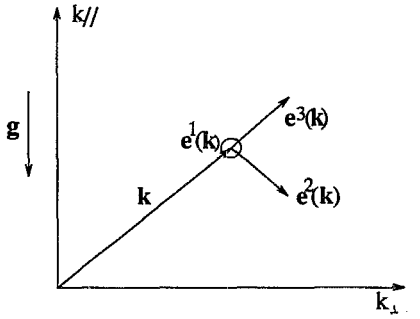

FIG. 2. The Craya–Herring orthonormal frame. The first vector of the frame comes out of the paper.

A. Craya–Herring frame

Any solenoidal (divergence free) velocity field in spectral space can be decomposed into two modes, that are orthogonal unit vectors in the plane normal to the wave vector $\mathbf{k}$, or:

$$\hat{u}_i=\hat{\varphi}^1 e_i^1+\hat{\varphi}^2 e_i^2,$$
$$\mathbf{e}^1(\mathbf{k})=(\mathbf{k}\times\mathbf{n})/|\mathbf{k}\times\mathbf{n}|, \tag{14}$$
$$\mathbf{e}^2(\mathbf{k})=(\mathbf{k}\times\mathbf{e}^1)/|\mathbf{k}\times\mathbf{e}^1|.$$

Of course, this definition uses an auxiliary (fixed) unit vector $\mathbf{n}$, chosen here, for convenience, as the vertical upward vector $n_i=-g_i/g=\delta_{i3}$, as shown in Fig. 2.

Accordingly, Eq. (4) for $\hat{\mathbf{v}}$ reads:

$$\hat{v}_i(\mathbf{k},t)=\hat{\varphi}^1(\mathbf{k},t)e_i^1(\mathbf{k})+\hat{\varphi}^2(\mathbf{k},t)e_i^2(\mathbf{k})+I\hat{\varphi}^3(\mathbf{k},t)e_i^3(\mathbf{k}). \tag{15}$$

For the reader who is not acquainted with spectral space, the above three terms decomposition can also be seen in physical space (see also Riley *et al.*[8]) as follows:

$$v_1=\frac{\partial\Psi'}{\partial x_2}+\frac{\partial\Phi}{\partial x_1}+\frac{\partial\Phi'}{\partial x_1},$$
$$v_2=-\frac{\partial\Psi'}{\partial x_1}+\frac{\partial\Phi}{\partial x_2}+\frac{\partial\Phi'}{\partial x_2}, \tag{16}$$
$$v_3=0+u_3+\frac{\partial\Phi'}{\partial x_3}.$$

In the above system of equations, each column corresponds to one of the spectral modes in (15); the third mode (with potential Φ') associated to the temperature field plays the same role as the dilatational velocity mode in the classical Helmholtz decomposition for compressible flows; the solenoidal part of $\mathbf{v}$ gives the actual velocity field $\mathbf{u}$ and is split into two solenoidal modes: the first mode (with potential Ψ') is the planar vortex flow. In general, it is not two-dimensional because Ψ' depends on the three space coordinates. By contrast, the two-dimensional mode (in a flow rotating around the vertical axis) is recovered in the limit $\partial/\partial x_3=0$ only [or $k_3=0$ in (15)] and, therefore, could be restricted to a subspace of measure zero. The second mode (with potential Φ) is associated with the vertical velocity; its solenoidal property is ensured by

$$\frac{\partial u_3}{\partial x_3}+\frac{\partial^2\Phi}{\partial x_1^2}+\frac{\partial^2\Phi}{\partial x_2^2}=0,$$

which corresponds to $\mathbf{e}^2\cdot\mathbf{k}=0$ in spectral space.

Of course, the derivation of Ψ', Φ, and Φ' and subsequent decomposition (16) for any given field $(\mathbf{u},\tau)$ involves integro-differential equations in physical space. This procedure is replaced by a simple geometric projection (on an orthonormal basis) in spectral space, which will only be used from now on.

From the linearized equation (5) for $\hat{\mathbf{v}}$

$$\frac{\partial\hat{v}_i}{\partial t}+L_{ij}\hat{v}_j=0 \tag{17}$$

the system of equations, in terms of $\hat{\varphi}^i$'s reads:

$$\frac{\partial\hat{\varphi}^1}{\partial t}(\mathbf{k},t)=0,$$
$$\frac{\partial\hat{\varphi}^2}{\partial t}(\mathbf{k},t)-Ne_3^2(\mathbf{k})\hat{\varphi}^3(\mathbf{k},t)=0, \tag{18}$$
$$\frac{\partial\hat{\varphi}^3}{\partial t}(\mathbf{k},t)+Ne_3^2(\mathbf{k})\hat{\varphi}^2(\mathbf{k},t)=0.$$

Now, statistical aspects can be re-introduced: for axisymmetric turbulence including reflectional symmetry (simplest symmetry consistent with background equations), the spectral tensor $\hat{V}_{ij}$ [Eqs. (7) and (8)] has only four nonzero components in $(\mathbf{e}^1,\mathbf{e}^2,\mathbf{e}^3)$:

$$\frac{1}{2}e_i^u\hat{V}_{ij}e_j^v=\begin{pmatrix}\Phi_1 & 0 & 0\\ 0 & \Phi_2 & \Psi^*\\ 0 & \Psi & \Phi_3\end{pmatrix} \tag{19}$$

directly linked to $\frac{1}{2}\langle\hat{\varphi}^{u*}\hat{\varphi}^v\rangle$ which depend on $k=|\mathbf{k}|$ and $\cos(\widehat{\mathbf{n},\mathbf{k}})=\cos\theta_k$. Each Φ_i, for $i=1,2,3$, is real and represents the different modes of the spectral density of energy (so-called "vortex," "wave," and "potential" after Riley *et al.*[8]). Ψ is complex and its real part generates the vertical buoyancy flux, according to:

$$\frac{1}{2}\langle u_3\tau\rangle=-\frac{N}{\beta g}\int\Psi_R\sin\theta_k d^3\mathbf{k} \tag{20}$$

with $\Psi=\Psi_R+I\Psi_I$. For the imaginary part of Ψ, we have $\int_k\Psi_I\sin\theta_k d^3\mathbf{k}=0$ due to symmetry. Additional constraints are $\Phi_1=\Phi_2$ and $\Psi=0$ for $\cos\theta=\pm1$ (polar isotropy) and finally $\Phi_i\geqslant 0$, $i=1,2,3$ and $\Phi_2\Phi_3-|\Psi|^2\geqslant 0$ (realizability).

The spectra defined above are governed by the following system of equations:

$$\left[\frac{\partial}{\partial t}+2\nu k^2\right]\Phi_1(\mathbf{k},t)=T^1(\mathbf{k},t),$$
$$\left[\frac{\partial}{\partial t}+2\nu k^2\right]\Phi_2(\mathbf{k},t)+N\sin\theta_k\Psi_R(\mathbf{k},t)=T^2(\mathbf{k},t),$$
$$\left[\frac{\partial}{\partial t}+2\nu k^2\right]\Phi_3(\mathbf{k},t)-N\sin\theta_k\Psi_R(\mathbf{k},t)=T^3(\mathbf{k},t), \tag{21}$$

$$\left[\frac{\partial}{\partial t}+2\nu k^2\right]\Psi_R(\mathbf{k},t)-2N\sin\theta_k[\Phi_2(\mathbf{k},t)-\Phi_3(\mathbf{k},t)]$$
$$=T^{\Psi_R}(\mathbf{k},t),$$
$$\left[\frac{\partial}{\partial t}+2\nu k^2\right]\Psi_I(\mathbf{k},t)=T^{\Psi_I}(\mathbf{k},t),$$

which corresponds, in the frame $(\mathbf{e}^1,\mathbf{e}^2,\mathbf{e}^3)$, to Eq. (8) in the fixed frame of reference; the right-hand sides are derived from the generalized transfer tensor T_{ij}. At this stage, the vortex mode is identified, but not the eigenmodes of gravity waves.

B. Eigenframe

The last step in our formal work is to use the eigenmodes of the linear regime. Looking at the fluctuating field, the system of Eqs. (18) is readily diagonalized:

$$\left[\frac{\partial}{\partial t}+\varepsilon INe_3^2(\mathbf{k})\right](\hat{\varphi}^{|\varepsilon|+1}+\varepsilon I\hat{\varphi}^3)=0,\quad \varepsilon=0,\pm1. \tag{22}$$

Thus, the solution of the linearized Eq. (17) reads:

$$\hat{\mathbf{v}}(\mathbf{k},t)\cdot\mathbf{N}^\varepsilon(\mathbf{k})=e^{-\varepsilon Ie_3^2(\mathbf{k})N(t-t_0)}\ \hat{\mathbf{v}}(\mathbf{k},t_0)\cdot\mathbf{N}^\varepsilon(\mathbf{k}),\quad \varepsilon=0,\pm1 \tag{23}$$

where

$$N_i^\varepsilon(\mathbf{k})=\left(e_i^{|\varepsilon|+1}(\mathbf{k})+\varepsilon\frac{k_i}{k}\right)\Big/\sqrt{|\varepsilon|+1}$$

is the eigenmode associated to the eigenvalue $-\varepsilon INe_3^2(\mathbf{k})=\varepsilon IN\sin\theta_k$ (θ_k is the orientation of the wave vector to the vertical).

From the equation which defines G used in Sec. II,

$$\hat{v}_i(\mathbf{k},t)=G_{ij}(\mathbf{k},t,t_0)\hat{v}_j(\mathbf{k},t_0) \tag{24}$$

(matrix that generates the kernel of linearized equations), it is found:

$$G_{ij}(\mathbf{k},t)=\sum_{\varepsilon\in\{0,\pm1\}}N_i^\varepsilon(\mathbf{k})N_j^\varepsilon(\mathbf{k})e^{I\varepsilon\sin\theta_kNt}. \tag{25}$$

There appears the phase [when multiplying (23) by the Fourier mode $\exp(I\mathbf{k}\cdot\mathbf{x})$]

$$\phi_w=\mathbf{k}\cdot\mathbf{x}\pm N\sin\theta_kt \tag{26}$$

of the gravity wave of frequency:

$$\omega_k=N\sin\theta_k \tag{27}$$

this last equation being the dispersion relation for internal gravity waves. The eigenmodes for the linear (wave) regime correspond to $\varepsilon=\pm1$ (ε indicates the polarity) and involve both velocity (through $\hat{\varphi}^2$) and temperature (through $\hat{\varphi}^3$). In addition, the planar vortex mode associated to $\hat{\varphi}^1$ is recovered for $\varepsilon=0$.

In terms of the eigenmode intensities $\xi_\varepsilon=\hat{\varphi}^{|\varepsilon|+1}+\varepsilon I\hat{\varphi}^3$, the background equation reads:

$$\left(\frac{\partial}{\partial t}+\nu k^2-\varepsilon IN\sin\theta_k\right)\xi_\varepsilon$$
$$=\sum_{\varepsilon\varepsilon'\varepsilon''}\int_{p+q=k}m_{\varepsilon\varepsilon'\varepsilon''}(\mathbf{k},\mathbf{p},\mathbf{q})\xi_{\varepsilon'}(\mathbf{p},t)\xi_{\varepsilon''}(\mathbf{q},t)d^3\mathbf{p}. \tag{28}$$

Using the new variable $\xi'_\varepsilon=\xi_\varepsilon\ e^{-\varepsilon INt\sin\theta}$ in the above equation and taking the limit of large N (or under a nondimensional form, at small Froude number), it can be seen that turbulence under stable stratification is governed by almost the same equation as free (neutral) turbulence, but the triads involved in its dynamics are restricted to *resonant* triads, such that:

$$\varepsilon\sin\theta_k+\varepsilon'\sin\theta_p+\varepsilon''\sin\theta_q=0 \tag{29}$$

(ε, ε', and ε'' can be equal to 0, +1, or −1). This argument was successfully used by Waleffe[21] in the case of rotating turbulence. Indeed, for nonresonant triads, the transfer is damped, at small Froude (or Rossby in the case of rotating turbulence) number. As shown below, our EDQNM2 model includes this property (see also Cambon and Jacquin[11] for rotating turbulence) but allows one to obtain good statistical results for a wider range of Froude and Reynolds numbers. The EDQNM procedure could be applied to the above nonlinear equation (for ξ_ε or ξ'_ε), but it is equivalent to start with equations in the fixed frame of reference (given in Sec. II) and to use Eq. (25) in the closure equation (12).

Looking at second order correlations, the left-hand side of Eq. (21) is readily diagonalized using the following four quantities:

$$\Phi_1,$$
$$\Phi_2+\Phi_3=\Phi_W \text{ total "wave" energy (kinetic+potential)}, \tag{30}$$
$$\Psi_I,$$
$$\Phi_2-\Phi_3+I\Psi_R\equiv\Phi_Z \text{ oscillating mode (see Table I)}.$$

The first three are conserved in the strict linear limit, whereas the last is affected by a phase $\exp(2INt\sin\theta)$. We recall that the Φ_i's and Ψ are the nonzero components of the covariance matrix in terms of the $\hat{\varphi}^i$'s (components of the vector $\hat{\mathbf{v}}$ in the Craya–Herring frame) which do not lead to diagonalizing the linearized equations. Only the $\langle\xi^*_\varepsilon\xi_{\varepsilon'}\rangle$ and related components ξ_ε allow one to achieve the diagonalization. Of course, the four quantities written above are related to the $\langle\xi^*_\varepsilon\xi_{\varepsilon'}\rangle$'s; for example, $\Phi_W=\Phi_2+\Phi_3=\langle\xi^*_{+1}\xi_{+1}\rangle+\langle\xi^*_{-1}\xi_{-1}\rangle$.

Looking at the third order correlations, closed by EDQNM2, Eqs. (12) and (25) yield an analytical integration in time

$$\int_{t_0}^t G_{jl}^{ED}(\mathbf{k},t,t')G_{pm}^{ED}(\mathbf{p},t,t')G_{qn}^{ED}(\mathbf{q},t,t')\,dt'$$
$$=\sum_{(\varepsilon,\varepsilon',\varepsilon'')\in\{0,\pm1\}^3}N_j^\varepsilon(\mathbf{k})N_l^\varepsilon(\mathbf{k})N_p^{\varepsilon'}(\mathbf{p})N_m^{\varepsilon'}(\mathbf{p})$$
$$\times N_q^{\varepsilon''}(\mathbf{q})N_n^{\varepsilon''}(\mathbf{q})\theta_{kpq}^{\varepsilon\varepsilon'\varepsilon''}(t) \tag{31}$$

with

$$[\theta_{kpq}^{\varepsilon\varepsilon'\varepsilon''}]^{-1}=\underbrace{\eta(k,t)+\eta(p,t)+\eta(q,t)}_{[\theta_{kpq}]^{-1}} -IN(\varepsilon \sin\theta_k+\varepsilon' \sin\theta_p+\varepsilon'' \sin\theta_q) \tag{32}$$

in the limit $t_0=-\infty$. At finite t_0, the above expression could be replaced by $(1-\exp([t_0-t]/\theta_{kpq}^{\varepsilon\varepsilon'\varepsilon''}))/\theta_{kpq}^{\varepsilon\varepsilon'\varepsilon''}$. The characteristic time obtained by this procedure explicitly depends on the stratification but for the resonant triads; hence, the transfer terms, which account for the nonlinearity in the dynamics of double correlations, will be significantly damped by the stratification, except for resonant triads. The detailed form of these transfer terms and their contributions called T^1, T^2, T^3, T^Ψ in (21) are not given here for the sake of brevity. (The complete set of equations along with their derivation are given by Cambon[16] and vanHaren.[6]) We only state that their derivation is straightforward from Eqs. (12), (13) and (25), and that an eightfold decomposition is suggested by Eq. (32), according to the values ±1 (wave) or 0 (vortex) of the "polarity indices" ε, ε', ε''. Briefly, these contributions are of the kind

$$T^{\varepsilon\varepsilon'\varepsilon''}(\mathbf{k},t)=\int_{k+p+q=0}\frac{S_{\varepsilon\varepsilon'\varepsilon''}(\mathbf{k},\mathbf{p},\mathbf{q},t)}{\theta_{kpq}^{-1}-IN(\varepsilon \sin\theta_k+\varepsilon' \sin\theta_p+\varepsilon'' \sin\theta_q)}\,d\mathbf{p}d\mathbf{q} \tag{33}$$

where the numerator of the integrand involves double correlations and known geometric factors. Even when using simpler versions (EDQNM1 and EDQNM0), where $N=0$ in the above expression, the eightfold splitting in terms of eigenmodes will be retained.

It is clear that our EDQNM2 model involves [through Eqs. (32) and (33)] the resonant condition (29) given by the weakly nonlinear theory. Nevertheless, two kinds of resonant triads should be distinguished:

(i) Pure vortical interactions with $\varepsilon=\varepsilon'=\varepsilon''=0$. For the corresponding term T^{000}, no geometric constraint is required in the triadic integral. In other words, all triads ($\mathbf{k}+\mathbf{p}+\mathbf{q}=\mathbf{0}$) are resonant when considering interactions involving only vortex modes.

(ii) Other interactions where at least one of the coefficients ($\varepsilon,\varepsilon',\varepsilon''$) is not zero, thus involving at least one wavy mode. The corresponding transfer term is restricted by geometric constraints (other than $\mathbf{k}+\mathbf{p}+\mathbf{q}=\mathbf{0}$) on the angles θ_k, θ_p, θ_q, and only particular shapes of triads, and also particular orientations of the plane that contains them, are resonant. This case, in the following referred to as resonant *gravity* waves, includes the condition:[30]

$$\mathbf{k}\pm\mathbf{p}\pm\mathbf{q}=0,$$

$$\omega_k\pm\omega_p\pm\omega_q=0$$

that is valid when a net exchange of energy in the interaction of three gravity waves $(\mathbf{k},\omega_k)$, $(\mathbf{p},\omega_p)$, $(\mathbf{q},\omega_q)$ occurs. The dispersion relation (27), plugged into this last equation, gives the condition (29) for a triad to be resonant with $\varepsilon=\pm1$, $\varepsilon'=\pm1$, $\varepsilon''=\pm1$.

Note that the resonance criterion for triadic interactions including vortex modes has also been established using a perturbation technique.[23]

IV. NUMERICAL RESULTS: THE CONSTRUCTION OF THE TRANSFERS

Equations of the model EDQNM2 are solved numerically in order to obtain the covariance matrix (19). The four scalar spectra Φ_1, Φ_2, Φ_3, $\Re(\Psi)=\Psi_R$ (real part of Ψ; its imaginary part $\Im(\Psi)=\Psi_I$ is ignored; it can be shown from the EDQNM2 equations that Ψ_I remains zero if it is zero initially) are discretized using 32 values of the wave number k and 19 values of the polar angle θ_k in the range $[0,\pi/2]$ for each k. The left-hand side of the system (21) of equations is taken into account implicitly in order to capture the linear regime with a maximum of accuracy. Nevertheless, the results are completely accurate only in the first two periods of Brünt–Väisälä, because of the angular integration (over discretized θ_k) of terms affected by the angular-dependent dispersion law (27) as shown by vanHaren.[6] In any case, the problem of angular inaccuracy would be worse in a DNS using a pseudo-spectral code (in which the number of discretized θ_k decreases with k), and this maximum elapsed time is sufficient to reach the qualitative features of the transfers, as discussed.

More details on the numerical procedure are also available in Ref. 6

For convenience, the EDQNM1 version [$N=0$ in the terms (33) involved in the right-hand side of (21)] and the EDQNM0 ($N=0$ in both the right- and the left-hand sides of (21)] version are numerically solved in the same conditions for the purpose of detailed comparisons.

A. Initial data and choice of parameters

In order to study how the anisotropy develops, the initial data are chosen strictly isotropic, so that:

$$\Phi_1=\Phi_2=E(k)/4\pi k^2;\quad \Phi_3=E^P(k)/4\pi k^2;\quad \Psi=0. \tag{34}$$

Previous DNS[19] were undertaken with zero initial potential energy ($E^P=0$). In the same situation, results of the EDQNM model (especially EDQNM1) were compared with DNS results.[31,6] Both DNS and EDQNM results showed how

the exchange of energy between the wave kinetic energy Φ_2 and the potential energy Φ_3 occurs in an oscillatory manner. These oscillations denote the role of the internal waves, without net direction of propagation. (In the case of one gravity wave, the fluid oscillates up and down. In stratified turbulence the flow can be regarded as a superposition of an infinite number of gravity waves propagating in every direction.)

During this alternating accumulation and release of potential energy, an irreversible anisotropy builds in, due to both linear and nonlinear interactions, which leads to an angular (with respect to the vertical) variation of the vortex kinetic energy Φ_1 and of the total wave energy $\Phi_W=\Phi_2+\Phi_3$ (both are nonoscillating quantities, which are easier to handle in the scope of a study of global tendencies during the temporal evolution).

It is important to notice that this resulting anisotropy is much different from the one given by linear dynamics for double correlations [cf. Rapid Distortion Theory (RDT)], in that the irreversible character of the former does not appear in the latter at all. In this respect, the predictions of EDQNM cannot be found using classical RDT. These preliminary results suggest to only look at how the angular dependence develops in Φ_1 and Φ_W, which are invariant in a pure linear and inviscid regime, and thus allow to characterize the irreversible anisotropy reflected by nonlinear interactions through specific spectral transfer terms T^1 and T^W.

The origin of this angular anisotropy is sought by looking at the detailed anisotropic transfers, in the next section. We can make sure that our results do not depend on the time at which the spectra are looked at, since the general shapes of the transfer curves for Φ_1 and Φ_W are preserved throughout all times; therefore it is sufficient to look at the transfers at a given time when the spectrum is well established.

Nevertheless, if $\Phi_2 \neq \Phi_3$, the linear dynamics influence the solution of system (21), and thus implicitly modify the history of the transfer terms T^1 and T^W through the closure model. Hence, we prefer to remove the "linear" strong oscillations, at least in the preliminary phase, by choosing, in addition to the isotropy, an initial equidistribution $\Phi_2=\Phi_3$ (or $E=E^P$), as already considered by Cambon.[16]

In any case, note that the "rapid" linear inviscid evolution leads to a trend towards equidistribution in average $\langle(\varphi^2)^2\rangle-\langle(\varphi^3)^2\rangle\to 0$ where $\langle(\varphi^i)^2\rangle=\int\Phi_i d^3\mathbf{k}$ as $(Nt)^{-1/2}$, as shown by vanHaren.[6]

Hence, our initial data seem to be convenient for emphasizing the rise of an irreversible behavior dominated by nonlinear effects. For this purpose, it is important to note that the EDQNM closure model allows one to obtain directly the spectrum of triple correlations from any given energy spectrum. Therefore, our present anisotropic computation starts with an initial energy spectrum already well developed (see Fig. 3), i.e., the analytical spectrum $E_0(k)$, defined below, has evolved during a precomputation using a classical analytically isotropic EDQNM closure model. The criterion for deciding when to stop this first period (which can be seen as a zone of negative times $[-t_0, 0]$ on a time scale where the Brünt–Väisälä frequency jumps from 0 to N at time $t=0$) is to go beyond the minimum of the kinematic time scale $\tau=k/\varepsilon$—ratio of kinetic energy to dissipation—and reach the point at which τ evolves linearly with time t. The main advantage of this procedure is to allow the triple correlations to reach the level of expected nonlinear trends much faster than for an anisotropic direct numerical simulation starting directly from the given analytical spectrum $E_0(k)$. The "isotropic precomputation" is started with the energy spectrum E_0 given by $E_0(k)=16(2/\pi)^{1/2}u_0^2k^4k_i^{-5}\exp(-2(k/k_i)^2)$ with $k_i=8$, as for 128^3 DNS and EDQNM initial data.[31,6]

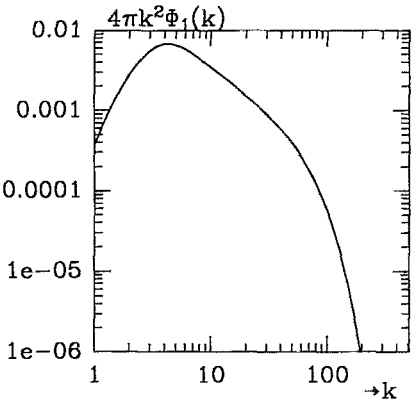

FIG. 3. The initial spectrum (time $t=0$) for both EDQNM1 and EDQNM2 calculations, developed from $E_0(k)$ by an isotropic EDQNM closure scheme.

The relevant nondimensional parameters for this study are the Froude and the Reynolds numbers. The Froude number $\mathrm{Fr}=(U/L)/N$ compares the characteristic time of the stratification (N^{-1}) to a turbulent turnover time $(L/U$, where U is a RMS velocity and L an integral length scale). At small Froude number, it is possible to separate a "rapid" time scale Nt from a slow one, so that only resonant triads evolve according to the slow time. At sufficiently large Froude number—$\mathrm{Fr}\geqslant 2$— stratification no longer affects the dynamics of freely decaying turbulence. The initial values of Fr and Re^λ (based on the Taylor microscale) are respectively around 0.23 and 60; the value of Re^λ is higher than the maximum allowed by a 128^3 DNS taking into account a complete spectrum, and Fr is not too small, so that our model is used far from the conditions of a weakly nonlinear approach.

B. Results

Figure 4 shows the evolution of the three modes of energy with nondimensional time $Nt/2\pi$:

(i) the vortex kinetic energy $\langle(\varphi^1)^2\rangle=\int\Phi_1 d^3\mathbf{k}$ smoothly decreases with time;

(ii) the wave kinetic and potential modes oscillate as they exchange energy, with an amplitude of oscillations more important in EDQNM2.

Figure 5 shows the Φ_1 and $\Phi_2+\Phi_3$ spectra after a time evolution $Nt/2\pi=1.5$, for EDQNM1 and EDQNM2. (The spectra are multiplied by $4\pi k^2$, first by reference to the integrated transfer spectrum over a sphere, but also to enhance the role of the medium wave numbers, in the inertial range.) The angular anisotropy is present for both models under the

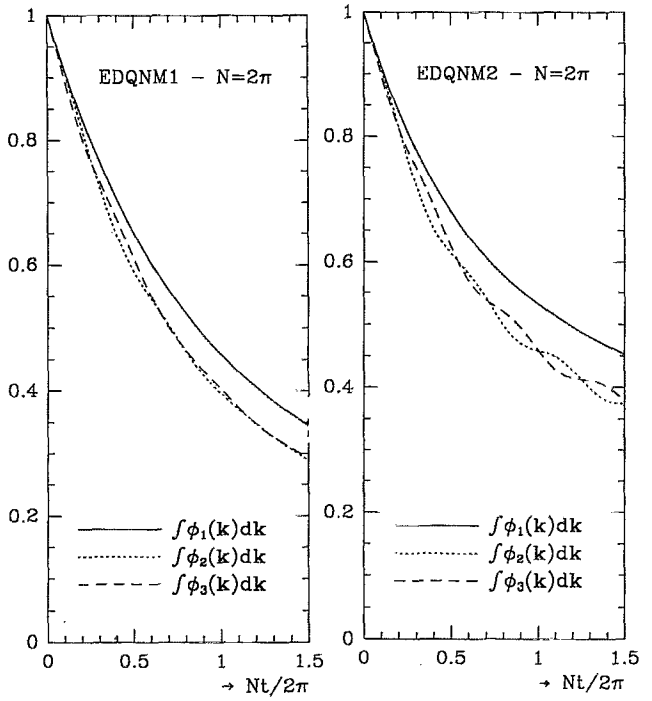

FIG. 4. Time evolution of the three energy modes (nondimensionalized by initial value)—vortex kinetic energy (integrated Φ_1 spectrum), wave kinetic energy (integrated Φ_2 spectrum) and wave potential energy (integrated Φ_3 spectrum)—for EDQNM1 and EDQNM2.

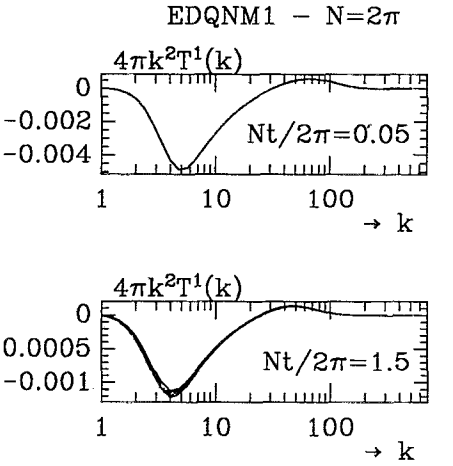

FIG. 6. EDQNM1 axisymmetric transfer evolution for the vortex kinetic energy Φ_1 at initial and final stages of calculation ($Nt/2\pi=0.05$ and 1.5).

form of an accumulation of energy around the pole ($\cos\theta_k=1$ or $\mathbf{k}\|\mathbf{g}$). However, it is much smaller in the case of EDQNM1 than in the case of EDQNM2; this comes from the big difference in the transfers for the two models. This is illustrated when looking at the time evolution of the energy transfers for EDQNM1 in Fig. 6 (where only the initial and final transfers are plotted, since the transfer evolves smoothly between those two stages) and comparing them with the EDQNM2 counterparts in Fig. 7. Not only the levels of the transfers are different, but also the very nature and origin of the anisotropy in these transfers. The shape of the transfer spectra do not vary with the angle θ_k for EDQNM1, whereas we get much different shapes in EDQNM2 along with a greater variability in time.

A good characterization of the conical structure in physical space induced by anisotropic spectra is the Moreau angle[17] defined by:

$$\cos^2\beta_{100}(t)=\frac{\int_{\mathbf{k}}\Phi_1(\mathbf{k},t)\cos^2\theta_k d\mathbf{k}}{\int_{\mathbf{k}}\Phi_1(\mathbf{k},t)d\mathbf{k}}$$

for the vortex energy spectrum, and by:

$$\cos^2\beta_{023}(t)=\frac{\int_{\mathbf{k}}(\Phi_2(\mathbf{k},t)+\Phi|_3(\mathbf{k},t))\cos^2\theta_k d\mathbf{k}}{\int_{\mathbf{k}}(\Phi_2(\mathbf{k},t)+\Phi_3(\mathbf{k},t))d\mathbf{k}}$$

for the wave total energy spectrum, following the terminology introduced by vanHaren.[6] In the case of isotropic spectra, the cosine of the Moreau angle is equal to 1/3; it takes the value 1 if the energy is accumulated at the pole ($\cos\theta=1$) and the value 0 if the equator ($\cos\theta=0$) contains all of the energy. The angle β_{lmn} can be seen as the angle of the cone that contains most of the energy of the given spec-

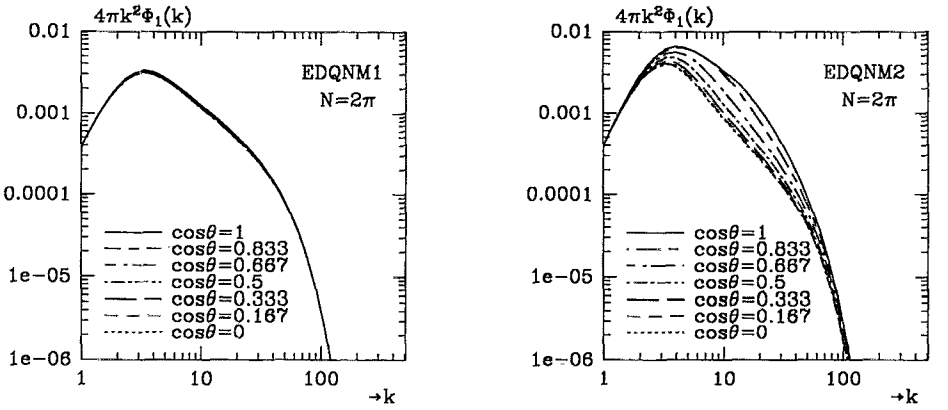

FIG. 5. EDQNM1 and EDQNM2 axisymmetric energy spectrum for the vortex kinetic energy Φ_1 at time $Nt/2\pi=1.5$ (in all the figures the following units are used: wave numbers in m^{-1} and $4\pi k^2$ times the energy or transfer spectra in m^3s^{-2}).

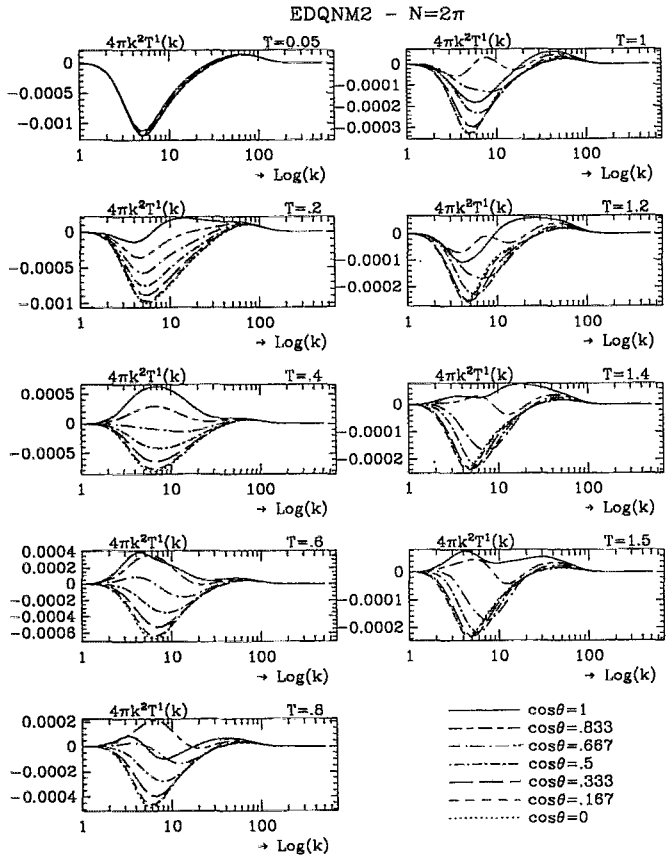

FIG. 7. EDQNM2 axisymmetric transfer evolution for the vortex kinetic energy Φ_1 for $Nt/2\pi \in [0.05, 1.5]$.

trum, and is therefore a good indicator in the situation we consider. Figure 8 shows the evolution of both $\cos \beta_{100}$ and $\cos \beta_{023}$ in time, for EDQNM2 spectra: they obviously start from 1/3, since the initial spectra are chosen to be isotropic, and increase progressively towards the value 1, which should only be attained asymptotically when t goes to infinity. The comparatively slight anisotropy generated by EDQNM1 would only lead to a small departure from 1/3 of the Moreau angles.

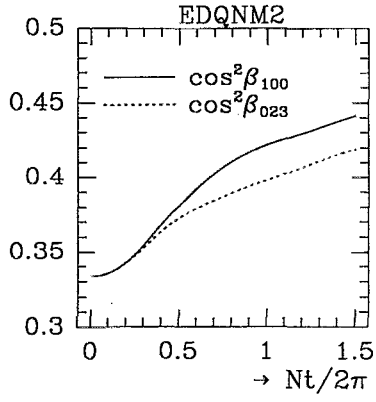

FIG. 8. Moreau angles for the vortex kinetic energy spectrum (β_{100}) and the total wave energy (β_{023}).

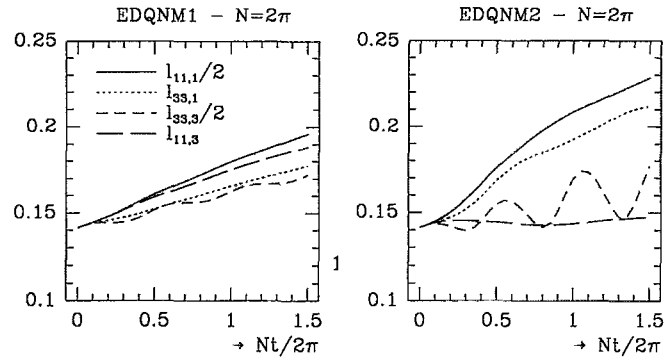

FIG. 9. Time evolution of the four relevant integral scales for the axisymmetric models: EDQNM1 and EDQNM2.

The corresponding trends in physical space are also considered, by looking at the time evolution of the integral scales $l_{11,1}$, $l_{11,3}$, $l_{33,1}$, and $l_{33,3}$; those four scales—which express the spatial correlation length along a given direction of one given component of the velocity field—are sufficient to characterize our axisymmetric flow [the axis of symmetry direction ($\|$) has been labeled 3, and the horizontal direction ($\perp$) 1]. For homogeneous anisotropic turbulence, the integral scales are computed using the second order spectral tensor $\hat{U}_{ij}(\mathbf{k},t)$ [kinematic part of $\hat{V}_{ij}$ in Eq. (7)], by the relation:

$$l_{ij,l}=\frac{\pi}{\langle u_i u_j\rangle}\int\int_{k_l=0}\hat{U}_{ij}(\mathbf{k},t)d^2\mathbf{k}$$

which leads to formulas for the integral scales computed from the different energy spectra;[6,11] for instance, the first one is given by:

$$l_{11,1}(t)=\frac{4\pi}{\langle u_1^2\rangle}\int_0^\infty k\left[\int_0^{\pi/2}\Phi_1(k,\theta_k,t)d\theta_k\right]dk.$$

Figure 9 shows those quantities for both EDQNM1 and EDQNM2. Our calculations deal with freely decaying turbulence, and accordingly, the integral scales gradually increase with time, which corresponds to the decrease of energy in the flow, after a possible short transition in case the turbulence were not completely developed. For an isotropic turbulence, all directions play the same role, and only one integral scale may be observed. In the case of the EDQNM1 model, the four integral scales show a slight difference in their evolution, with $l_{33,3}$ oscillating a little. Whereas in EDQNM2, it is remarkable that $l_{11,1}$ and $l_{33,1}$ increase a lot, which means that the flow gets layered and that the contribution from large scales to the energy is more important in the horizontal direction than in the vertical direction. Accordingly, the vertical scale $l_{11,3}$ almost remains constant, since the vertical exchanges of energy are reduced a lot. Finally, $l_{33,3}$ presents strong oscillations around a mean value that very slowly increases. These strong oscillations reflect the fact that $\langle u_3^2\rangle l_{33,3}$ takes into account the "equatorial" ($k_3=0$) distribution of the "wave" mode Φ_2, where the frequency $N \sin \theta_k$ is maximum.

In the EDQNM1 model, the anisotropic effect of stratification is indeed linear dynamics, which can be retrieved in

TABLE II. The eight forms of the characteristic time $\theta_{kpq}^{\varepsilon\varepsilon'\varepsilon''}$.

$\varepsilon'\varepsilon''$	00	01
ε		
0	$\frac{1}{\eta_{kpq}}$	$\frac{1}{\eta_{kpq}-IN\varepsilon''\sin\theta_q}$
1	$\frac{1}{\eta_{kpq}-IN\varepsilon\sin\theta_k}$	$\frac{1}{\eta_{kpq}+IN(\varepsilon\sin\theta_k+\varepsilon''\sin\theta_q)}$
$\varepsilon'\varepsilon''$	10	11
ε		
0	$\frac{1}{\eta_{kpq}-IN\varepsilon'\sin\theta_p}$	$\frac{1}{\eta_{kpq}-IN(\varepsilon'\sin\theta_p+\varepsilon''\sin\theta_q)}$
1	$\frac{1}{\eta_{kpq}-IN(\varepsilon\sin\theta_k+\varepsilon'\sin\theta_p)}$	$\frac{1}{\eta_{kpq}-IN(\varepsilon\sin\theta_k+\varepsilon'\sin\theta_p+\varepsilon''\sin\theta_q)}$

the RDT approximation, if $\Phi_2 \neq \Phi_3$ initially. In this case, the set of Eqs. (21) shows that Ψ_R is affected by the difference $(\Phi_2-\Phi_3)$ in proportion of $2N\sin\theta_k$, and therefore the linear dynamics for Φ_2 and Φ_3 correspond to oscillations. Considering the isotropic with $\Phi_2=\Phi_3$ initial conditions, it is necessary that the nonlinear transfer give different initial slopes to the evolution of Φ_2 and Φ_3, in order to get linear anisotropic tendencies at all.

From the latter initial state, the EDQNM2 transfers evolve in two steps: first the anisotropy builds, and the transfers are accordingly mainly *angular* transfers; second, some side effects of stratification appear, and the transfers evolve to a cascade in wave-number space, still retaining their anisotropic characteristics. After this turning point, the maximum of the transfer in EDQNM2 is noticeably smaller than in Fig. 6. The last point is illustrated by the evolution of the three energy modes in Fig. 4, where one notices a reduction of the decrease slope of EDQNM2 compared to EDQNM1.

V. DETAILED INTERACTION TRANSFER TERMS

The expression for the transfer term shows that the damping is different depending on the mode (vortex: $\varepsilon=0$ or wave: $\varepsilon=\pm1$) chosen for each wave vector as shown in Table II. In any case, if $\varepsilon=0$ or $\varepsilon=\pm1$, it is the contribution respectively to the vortex or wave part of the total transfer which is calculated [respectively $T^1(\mathbf{k})$ and $T^W(\mathbf{k})=(T^2+T^3)(\mathbf{k})$]. Hence, amongst the eight possible interactions—which we determine by the binary number $(|\varepsilon||\varepsilon'||\varepsilon''|)$—, the (000) interaction for example, shows the part $T^{(000)}$ of the vortex transfer at $\mathbf{k}$ due to vortex interactions at $\mathbf{p}$ and $\mathbf{q}$. (Note that *vortex* and *wave* are used in the context of the Craya decomposition for the pure linear regime, but there are some limitations in the real meaning of this terminology,[23] especially when one wants to interpret the results back in physical space.) In the following section we examine the detailed transfer terms, and especially the pure vortex one.

A. Contributions to the vortex transfer

There are only four transfer contributions to the vortex kinetic energy Φ_1, coming from triads in which $\varepsilon=0$, so that we only look at $(\varepsilon\varepsilon'\varepsilon'')\in\{(000),(001),(010),(011)\}$. Figure 10 shows them all at time $Nt/2\pi=1.5$ given by the EDQNM2 model. Strikingly, the pure vortex (000) interaction seems to be mainly responsible for the anisotropy of Φ_1. Indeed, its isotropic EDQNM0 equivalent already contains some of the "anisotropic" features that can advect energy throughout angular space. Figure 11 shows how, for all three different EDQNM models, the transfer is negative at the equator ($\cos\theta=0$) and positive around the pole ($\cos\theta=1$). However, for EDQNM0, the complete transfer term on Φ_1 is, of course, isotropic since the transfer terms (001), (010), and (011) compensate the (000)'s anisotropy.

But when looking at the EDQNM2 model, we first see that:

(i) The levels of the transfers on the (000) term are lowered (which is partly explained by the fact that after the same evolution time, the Φ_1 and $\Phi_2+\Phi_3$ modes have energy levels higher for EDQNM0).

(ii) The shape of the (000) transfer term—even though it is a bit distorted—is very much like its isotropic counterpart.

The time $Nt/2\pi=0.4$ at which the three transfers are plotted on Fig. 11 roughly corresponds to the time at which the total transfer on Φ_1 begins to play the role of advecting energy towards the pole, as can be noticed in Fig. 7. During a small period, the shape of the EDQNM2 $T^{(000)}$ term remains close to that of the EDQNM0 one, but when the spectrum becomes more variable with θ_k, its shape departs more from the isotropic equivalent.

The origin of the anisotropy in the total EDQNM2 transfer may be due to the pure vortex (000) interaction term. It is seen in Fig. 11 that this part of the transfer creates the anisotropy in the energy containing range, and at the beginning of the evolution, the remaining terms (001)(010)(011) react by building a partly balancing anisotropic transfer. But they fail to make up for the whole originating anisotropy and the result is that the total transfer still contains a part of the anisotropy induced by the pure vortex interaction. Figure 12 shows, in this respect, the transfer spectra for $T^{(000)}$, $T^{(001)}+T^{(001)}+T^{(010)}$ and $T^1=T^{(000)}+T^{(001)}+T^{(001)}+T^{(010)}$, that confirms this result.

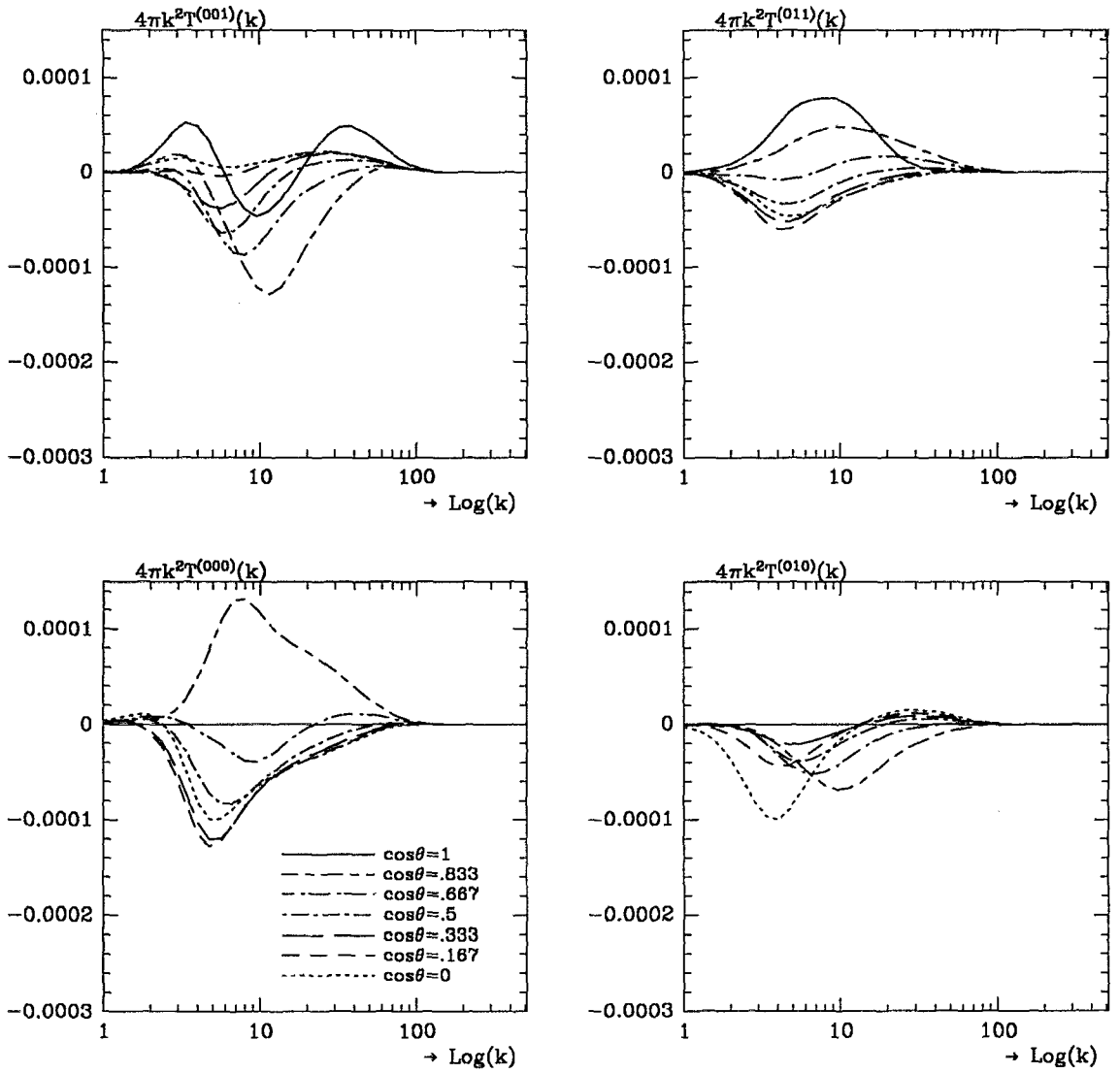

FIG. 10. All four interactions contributing to the EDQNM2 transfer of energy on Φ_1 at time $Nt/2\pi=1.5$, with $N=2\pi$.

On the EDQNM1 curves (Fig. 13), it is clear that the transfer shapes of $(T^{(001)}+T^{(010)}+T^{(011)})(\mathbf{k})$ are very much similar to the isotropic transfer, but for the pure anisotropy generated by the $T^{(000)}$ interaction transfer. Hence, the total transfer of Φ_1, the sum of the two, is very close to the isotropic one, except for a small angular advection.

Note how the transfer at the pole is identically zero for $T^{(000)}$: the global Φ_1 transfer at $\cos\theta=0$ is therefore only generated by vortex/wave interactions, which primarily set the level of the polar transfer, and the pure vortex interaction redistributes the levels of the transfers away from the pole. This particular role of the polar transfer is also seen on the curves given for EDQNM2. These plots show that $T(\mathbf{k})$, even though far from the isotropic spectral shape of the energy transfer, is still transferring energy towards the pole, and the generation of this phenomenon comes, as for EDQNM1, mainly from the pure vortex interaction.

This tendency, compared to the results given by the EDQNM with solid body rotation,[11] confirms the above conclusions, associated with the fact that the selection of resonant triads which include waves do not bring out significant transfer levels, which shows their relatively small importance in the global transfer—as we shall see in the next section.

B. Resonant triads which involve gravity waves

For the (000) term, the characteristic time $\theta_{kpq}^{\varepsilon\varepsilon'\varepsilon''}$ is independent of the orientation θ_k, which explains the similarity with the isotropic transfer. But when $\varepsilon' \neq 0$ or $\varepsilon'' \neq 0$, then $\theta_{kpq}^{\varepsilon\varepsilon'\varepsilon''}$ is changed depending on the value of $\sin\theta_p+\sin\theta_q$ or only $\sin\theta_p$ or $\sin\theta_q$. For instance, if $\sin\theta_p+\sin\theta_q=0$, the triad $\mathbf{k}$, $\mathbf{p}$, $\mathbf{q}$ has the same characteristic time as its isotropic equivalent. On the contrary, if $\sin\theta_p+\sin\theta_q\neq 0$, then the complex part of the characteristic time plays a role, and there is a phase scrambling.

The effect of the term $\theta_{kpq}^{\varepsilon\varepsilon'\varepsilon''}$ in EDQNM2 is to *select* some triads of somewhat more importance than others, depending on their frequency, which is directly linked to the angle θ to the vertical. In order to quantify their relative importance, we have carried out a series of calculations using

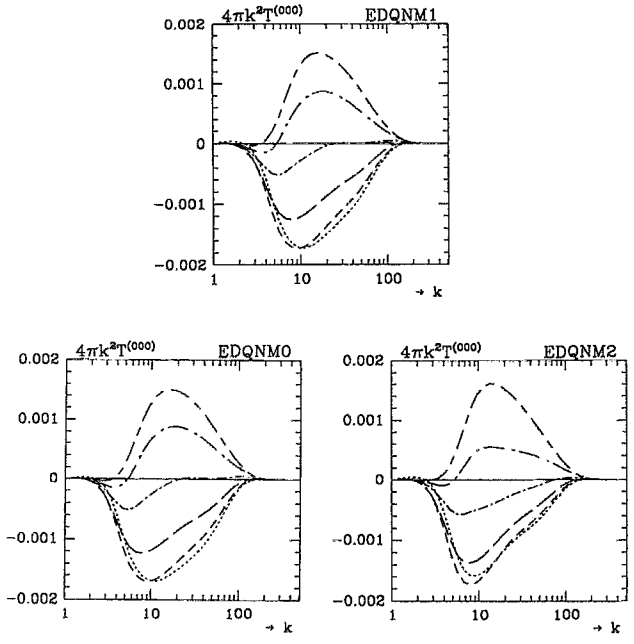

FIG. 11. Pure vortex interaction transfer term at time $Nt/2\pi=0.4$ (for the three models).

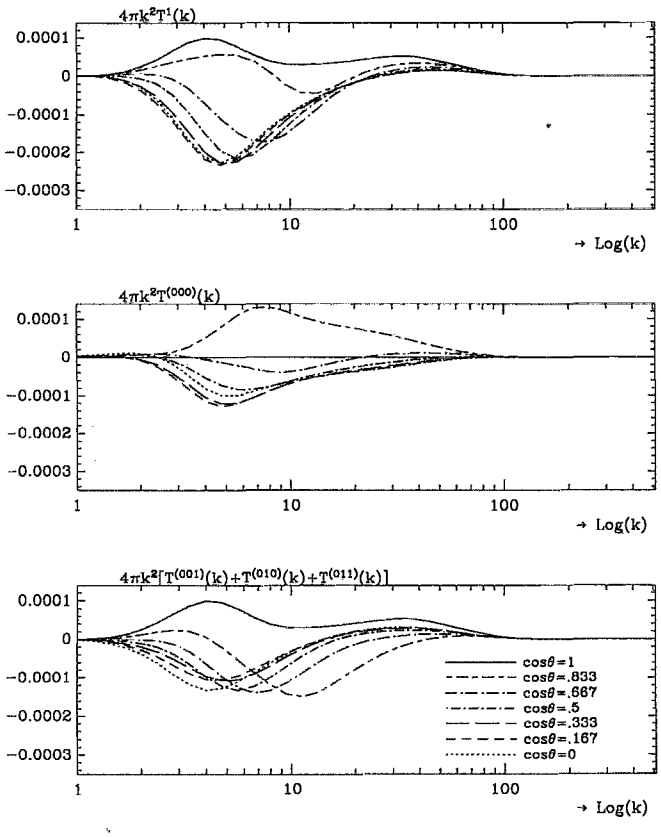

FIG. 12. Compared plots of the pure vortex interaction contributing to Φ_1 transfer, and the sum of the three other terms, along with the total transfer (at time $Nt/2\pi=1.5$), given by EDQNM2 calculations with $N=2\pi$.

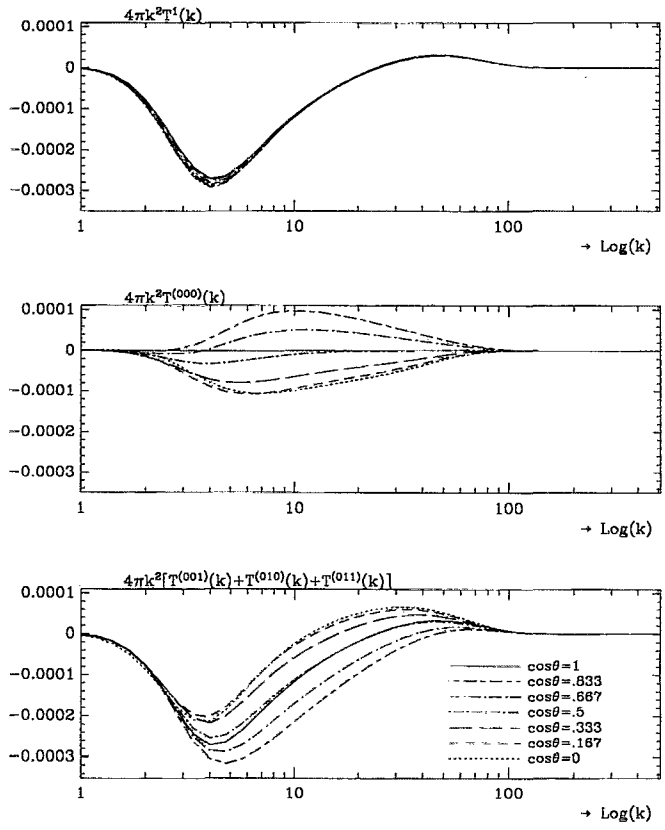

FIG. 13. Compared plots of the pure vortex interaction contributing to Φ_1 transfer, and the sum of the three other terms, along with the total transfer (at time $Nt/2\pi=1.5$), for EDQNM1 ($N=2\pi$).

a selection of resonant triads only. The results are presented hereafter, where a triad has been supposed to be resonant if:

$$\varepsilon \sin \theta_k+\varepsilon' \sin \theta_p+\varepsilon'' \sin \theta_q \leqslant \zeta \tag{35}$$

(ζ is being varied to see its influence on the result and on a possible interpretation, but cannot be taken exactly equal to zero, since our decomposition of spectral space is not continuous). Therefore, whenever the lower part of the characteristic time has a (almost) zero imaginary part, we select the corresponding triad, which is then assumed to be resonant, at a precision ζ. Note that we did *not* compare the relative values of the imaginary and real parts, which would lead to selecting the only triads that contribute a lot to the scrambling in angular space (i.e., for which the damping departs much from the basic isotropic damping $1/\eta_{kpq}=\theta_{kpq}$).

As we have previously mentioned, the results of this selection show that the transfers associated to the resonant wave triads are very low compared to the global transfer, as shown in Fig. 14. In this respect, the process of selecting resonant triads is not exactly the one that generates directly the anisotropy, and is definitely not sufficient for this generation.

The resonance selected transfers are plotted on Fig. 14. For T^1, the only significant remaining terms are, of course $T^{(000)}$—consistent with the fact that *all* triads involving three vortex modes are resonant (see Ref. 23)—but also the transfer due to contributions from wave/wave interactions; this

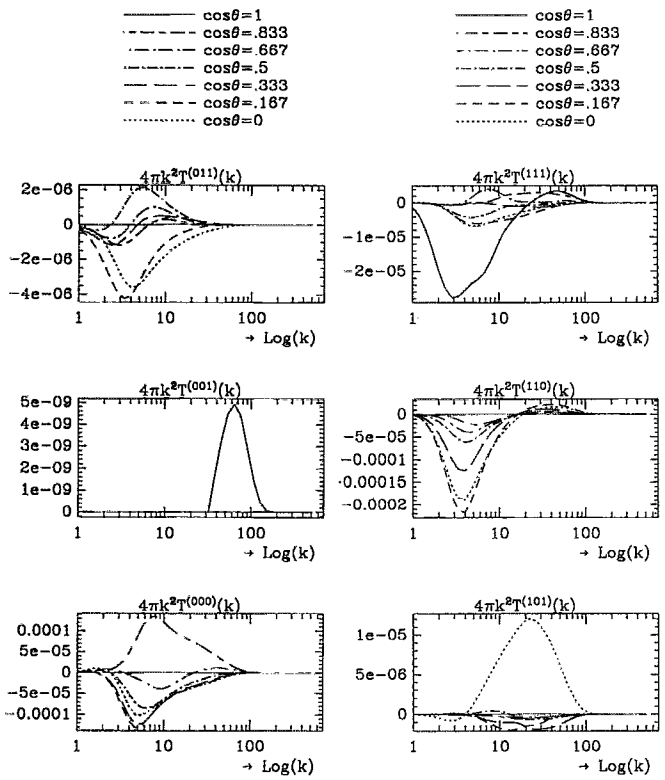

FIG. 14. Φ_1 and $\Phi_2+\Phi_3$ transfer contributions due to resonant triads only (with an accuracy of the selection on the sines of $\zeta=1/33$), for EDQNM2, at $N=2\pi$. The transfers $T^{(010)}$ and $T^{(100)}$ are not presented, since their part coming from resonant triads vanish.

one contributes also to the polar accumulation of energy, with its level at $N=2\pi$ nearly twice that at $N=\pi$.

C. Contributions to the wave transfer

For the total wave energy $\Phi_2+\Phi_3$, the transfer coming from two vortex interactions vanishes immediately, and the contribution comes from the three remaining terms. The two mixed (i.e., wave/vortex) contributions act as if they were the ones that transfer energy from large scales towards smaller ones, at a rate maximal at the equator.

The four different interactions that contribute to the total wave energy transfer are plotted on Fig. 15. It is immediately seen that the transfer arising from two vortex modes associated to wave vectors $\mathbf{p}$ and $\mathbf{q}$ is much less than the three other ones. However, no obvious angular advection of energy is attributed to a specific kind of interaction as done in the vortex transfer.

Therefore, the anisotropy of the wave energy spectrum may come, at small Froude numbers, from nonlinear interactions between the vortex and wave energies. Figure 4 shows that Φ_1 somehow oscillates at $N=2\pi$, which is a clue for the above-mentioned interaction. Moreover, the axisymmetry hypothesis imposes that Φ_1 be equal to Φ_2 at the pole, since in this situation no privileged horizontal direction exists. Thus, if the vortex energy spectrum accumulates at the pole, it also drains, by this mechanism, the wave kinetic energy towards the pole.

VI. CONCLUSION AND PERSPECTIVES

The analysis done above about the origin of the anisotropy is expected to provide valuable information about the behavior of the wave and vortex fields in a stratified turbulent flow. A lot of detailed plots of the various transfer spectra have been shown; even though they are only a small part of the results that can be presented, they already provide many answers to questions about the originating anisotropy in the energy spectra, which is brought to light by many indicators, such as the Moreau angles or the integral length scales, apart from looking directly at the detailed spectra distributions.

First, the quite unexpected fact that the transfer term linked to the pure vortex interaction even in the isotropic case contains all the qualitative anisotropic features of the flow under stratification has been seen. Without stratification, the anisotropic shape of all other transfer contributions would exactly balance this anisotropy, so that the isotropy of the energy spectra is preserved.

Then, the resonant wave interactions, which had been suspected to have much influence on the transfers, are shown to have a very limited effect. In this calculation, the EDQNM2 model has been used profitably to investigate interaction processes between wave and vortex modes associated to a wave number. Therefore, quantitative results about energy transfers between the two fields are obtained, and simple mechanisms identified, looking at the angular dependence in spectral space. Of course, the contribution from nonresonant interactions is decreasing with the Froude number and subject to a rapid decay, in accordance with a phase scrambling. It is to be noted that the initial conditions were chosen isotropic and equipartitioned (same spectrum for the vortex kinetic energy as for the potential energy) in order to emphasize the role of the nonlinear interactions compared with the linear ones. The EDQNM1, which does not take into account the explicit effect of stratification in the third order correlations, performed well for initial zero potential energy, but is shown in this case to reflect poorly the irreversible anisotropic tendency of the flow.

It is possible now to summarize the most significant feature of the transition from 3-D isotropic turbulence under the effects of either strong rotation or strong stratification to an anisotropic state. The case of quasigeostrophic turbulence, in which both rotation and stratification are present, could be revisited in light of present analysis.

In the case of pure rotation, the geostrophic mode (or equivalently the steady eigenmode of the linear regime) is reduced to a pure 2-D contribution, ($k_3=0$ or $\partial/\partial x_3=0$) and represents a subspace of measure zero in quasi-isotropic 3-D turbulence. The emergence of a pure 2-D dynamics from the whole turbulent field dominated by inertial waves ($k_3\neq 0$) cannot be predicted without explicitly investigating nonlinear wave interactions. At low Rossby number, but not too small, the resonant interactions of inertial waves ($\cos\theta_k\pm\cos\theta_p\pm\cos\theta_q=0$), including also triads of pure 2-D modes, play an essential role for concentrating the spectral energy towards $\cos\theta_k=k_3/k=0$ (Refs. 11 and 22) and, therefore, for increasing the "population of possible 2-D modes." The contribution of pure 2-D triadic interactions

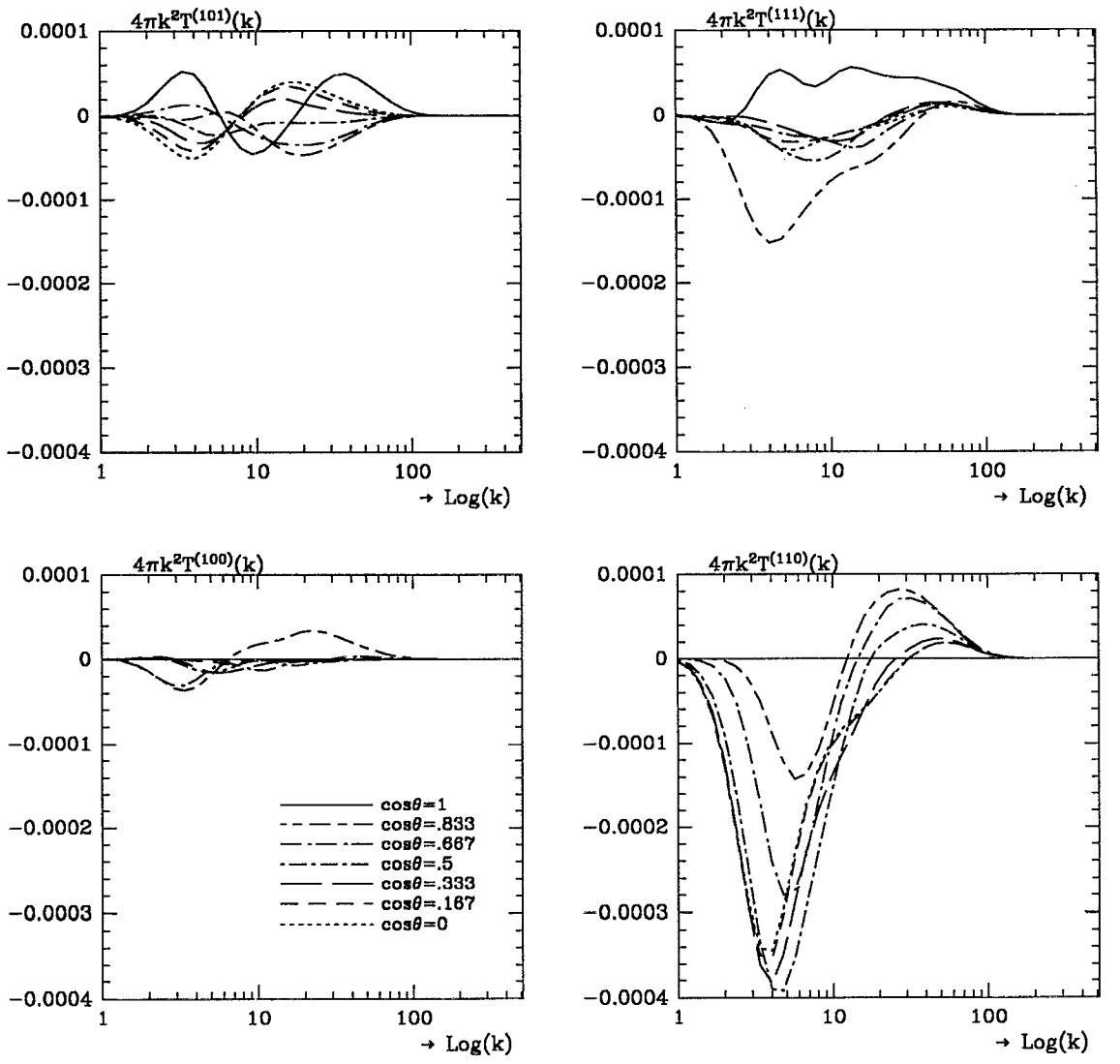

FIG. 15. All four contributions to the wave energy transfer, given by EDQNM2 at $Nt/2\pi=1.5$.

($\cos\theta_k=\cos\theta_p=\cos\theta_q=0$), however, remains weak with respect to the contribution of all the resonant interactions, which is itself weak compared to all triads, at least at low Rossby numbers and starting from strictly isotropic initial data. If quasi-2-D large eddies are present in the initial data (explicitly introduced[32] or even due to the lack of resolution and insufficient sampling of the initial DNS or LES fields), a pure 2-D dynamics with inverse energy cascade can accelerate the transition process. Another important effect for two-dimensionalization in this case, is the damping of 3-D small-scale turbulence in the presence of large quasi-2-D eddies under rotation, according to centrifugal stability criteria (Rayleigh; Bradshaw–Richardson) and "exact" stability analyses (see Ref. 33 for a review).

In the case of pure stratification, the geostrophic mode is the "vortex mode," whose energy represents *half* the total kinetic energy in isotropic 3-D turbulence (because $\Phi_1=\Phi_2$). Accordingly, the pure vortex–vortex interactions are initially important among all the nonlinear interactions. Our present computations confirm that the weight of resonant "waves" interactions is small at small Froude number with respect to these dominant vortex–vortex interactions. The latter tend to concentrate the spectral energy along vertical wave vectors (polar zone). In such a conical shape (see Fig. 1), opposite to that found in the case of pure rotation, both velocity and vorticity fields are quasihorizontal (since $\mathbf{k}\cdot\hat{\mathbf{u}}=0$ and $\mathbf{k}\cdot\hat{\boldsymbol{\omega}}=0$) but the transfer involves an increasing amount of triads with sides close to the vertical direction, and all tendency towards 2-D dynamics and inverse energy cascade is excluded. The conical structure in spectral shape and subsequent blocking of inverse cascade is linked to a strong dissipation by a turbulent shear induced by strongly decorrelated (in the vertical direction) "pancake" structures in physical space. The integral scales with vertical separation ($l_{11,3}$ and $l_{33,3}$ in Fig. 9) give a statistical measure of the thickness of these layers.

It may be pointed out that the angular dependence in spectral space remains the clue for understanding the dynamics, and not the difference between $\langle(\varphi^1)^2\rangle$ and $\langle(\varphi^2)^2\rangle$ (averaged energy). One could be tempted to interpret the

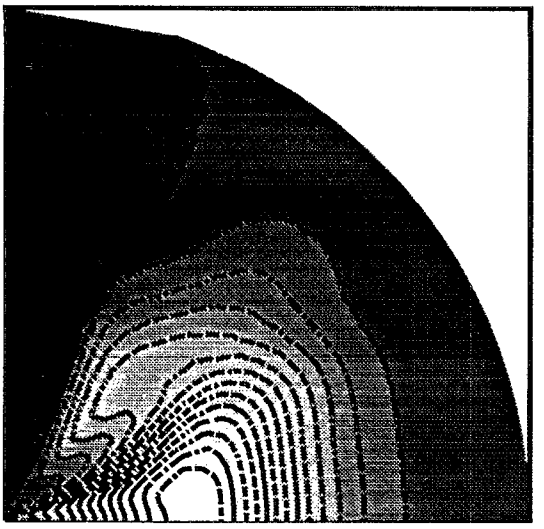

FIG. 16. The net kinetic energy transfer (T^1+T^2) on a $(k_\perp, k_\parallel)$ representation at time $Nt/2\pi=1.5$. The logarithmic contour range from -1.1×10^{-5} to 4.2×10^{-6} with dashes for negative values of the transfer. The area of maximum transfer is black and the minimum white.

horizontal layering as the effect of an inverse energy cascade (of two-dimensional turbulence) for velocity structures in the horizontal direction, but the relative concentration of spectral energy towards vertical wave vectors allows us to definitely exclude that assumption. Regarding the angular-dependent distribution, preliminary comparisons with DNS data were made by Teissèdre and Dang[32] and vanHaren[6] using also an original way of processing data for extracting angular-dependent spectral information from DNS or LES. These comparisons must be continued. For example, an alternative way of representing the map of nonlinear transfer rates of kinetic and potential energy is to plot their isolines versus the horizontal $(k_\perp)$ and vertical $(k_\parallel)$ components of the wave vector, as done by Ramsden and Holloway[26] for 3-D and 2-D DNS with gravity, to be compared with our present results shown in Fig. 16 for instance. This latter representation is applied to exactly the same EDQNM2 results as for Fig. 7, but it displays nonisotropic trends in a different manner.

Regarding continuation towards long-time computations, at high Reynolds number, asymptotic power laws in terms of the "rapid" time scale Nt, the Froude number, and a slow time scale based on the low wave number shape of the initial energy spectrum were proposed by Chasnov;[34] these asymptotic scaling laws especially take into account the strong difference between length scales with horizontal $(l_{.,1})$ and vertical $(l_{.,3})$ separation (illustrated by Fig. 9) and ought to be compared with LES and our EDQNM2 model.

Another logical continuation of this study will be to use this information in order to build a one-point model that may reproduce the behavior of stratified inhomogeneous flows. Of particular interest is the coupling between wave and vortex parts of the velocity field. Uittenbogaard and Baron[15] have proposed such a model using many approximations to simplify the equations. The new processes identified in our paper highlight different features, giving birth to different ideas for simplified quasi-isotropic EDQNM models or for a one-point closure model.

For example, as the pure vortical interaction has been shown to generate almost all the anisotropic trends, a physical model may only take into account the damping of the vertical energy exchange due to vortical modes. The other kinds of interactions, involving waves, may be dropped (or affected by a coefficient decreasing with the Froude number), as well as the effect of phase scrambling due to the waves, which is less important for a simple closure model. Such a simplification will allow one to get a model simple enough to be used for advanced inhomogeneous calculations, but also for engineering purposes.

ACKNOWLEDGMENTS

The authors wish to thank the referees for their criticisms and suggestions on the original manuscript. Also, thanks to Dr. vanHaren who has helped considerably in improving the presentation of this paper.

[1]E. J. Hopfinger, "Turbulence in stratified fluids: A review," J. Geophys. Res. **92**, 5287 (1987).
[2]C. Cambon and F. S. Godeferd, "Inertial transfers in freely decaying, rotating, stably stratified and MHD turbulence," in *Proceedings of The Seventh Beer-Sheva International Seminar on MHD Flows and Turbulence*, 14–18 February 1993 (AIAA, Washington, DC, in press).
[3]W. C. Reynolds, Lecture at the Euromech 288, 1992, Ecole Centrale de Lyon.
[4]S. H. Derbyshire and J. C. R. Hunt, "Structure of turbulence in stably stratified atmospheric boundary layers; comparison of large eddy simulations and theoretical models," in Proceedings of the 3rd IMA Conference on Stably Stratified Flows, *Waves and Turbulence in Stably Stratified Flows*, edited by S. D. Mobbs (Clarendon, Oxford, 1991).
[5]J. C. R. Hunt, D. D. Stretch, and R. E. Britter, "Length scales in stably stratified turbulent flows and their use in turbulence models," *Proceedings of the IMA Conference on Stably Stratified Flow and Dense Gas Dispersion*, edited by J. S. Puttock (Clarendon, Oxford, 1988), pp. 285–322.
[6]L. vanHaren, "Étude théorique et modélisation de la turbulence en présence d'ondes internes," Thèse de Doctorat, École Centrale de Lyon, January 1993.
[7]S. A. Orszag, "Analytical theories of turbulence," J. Fluid Mech. **41**, 363 (1970).
[8]J. J. Riley, R. W. Metcalfe, and M. A. Weisman, "Direct numerical simulations of homogeneous turbulence in density-stratified fluids," in *Proceedings of AIP Conference on Nonlinear Properties of Internal Waves*, edited by B. J. West (American Institute of Physics, New York, 1981), pp. 79–112.
[9]C. Cambon, "Étude spectrale d'un champ turbulent incompressible, soumis à des effets couplés de déformation et de rotation imposés extérieurement," Thèse d'État, Université de Lyon, 1982.
[10]G. Holloway and M. C. Hendershot, "Statistical closure for nonlinear Rossby waves," J. Fluid Mech. **82**, 747 (1977).
[11]C. Cambon and L. Jacquin, "Spectral approach to non-isotropic turbulence subjected to rotation," J. Fluid Mech. **202**, 295 (1989).
[12]N. N. Mansour, C. Cambon, and C. G. Speziale, "Theoretical and computational study of rotating isotropic turbulence," in *Studies in Turbulence*, edited by T. B. Gatski, S. Sarkar, and C. G. Speziale (Springer-Verlag, Heidelberg, 1991).
[13]L. Jacquin, O. Leuchter, C. Cambon, and J. Mathieu, "Homogeneous turbulence in the presence of rotation," J. Fluid Mech. **220**, 1 (1990).
[14]G. F. Carnevale and J. S. Frederiksen, "A statistical dynamical theory of strongly nonlinear internal gravity waves," Geophys. Astrophys. Fluid Dyn. **23**, 175 (1983).
[15]R. E. Uittenbogaard and F. Baron, "A proposal: extension of the $q^2-\epsilon$ model for stably stratified flows with transport of internal wave energy," Seventh Symposium on Turbulent Shear Flows, Stanford University, Stanford, 21–23 August 1989.
[16]C. Cambon, "Spectral approach to axisymmetric turbulence in a stratified

fluid," *Advances in Turbulence 2* (Springer-Verlag, Berlin, 1989).
[17]R. Moreau, "On magnetohydrodynamic turbulence," Proceedings of Symposium on Turbulence of Fluid and Plasma, Polytechnic Institute of Brooklyn, 1968, pp. 359–372.
[18]C. Cambon, L. Jacquin, and J. L. Lubrano, "Toward a new Reynolds stress model for rotating turbulence," Phys. Fluids A **4**, 812 (1992).
[19]O. Métais and J. R. Herring, "Numerical simulations of freely evolving turbulence in stably stratified fluids," J. Fluid Mech. **202**, 117 (1989).
[20]J. R. Herring, "Statistical theory of two- and quasi two-dimensional turbulence," Euromech 105, Grenoble, 6–8 September 1978.
[21]F. Waleffe, "Inertial transfer in the helical decomposition," Phys. Fluids A **5**, 677 (1993).
[22]P. Muller, G. Holloway, F. Heney, and N. Pomphrey," Nonlinear interactions among internal gravity waves," Rev. Geophys. **24**, 493 (1986).
[23]M. P. Lelong and J. Riley, "Internal wave-vortical mode interactions in strongly stratified flows," J. Fluid Mech. **232**, 1 (1991).
[24]G. Holloway, "On the spectral evolution of strongly interacting waves," Geophys. Astrophys. Fluid Dyn. **11**, 271 (1979).
[25]G. F. Carnevale and P. C. Martin, "Field theoretical techniques in statistical fluid dynamics: With application to nonlinear wave dynamics," Geophys. Astrophys. Fluid Dyn. **20**, 131 (1982).
[26]D. Ramsden and G. Holloway, "Energy transfers across an internal wave-vortical mode spectrum," J. Geophys. Res. **97**, 3659 (1992).
[27]A. Craya, "Contribution à l'analyse de la turbulence associée à des vitesses moyennes," Publ. Sci. Tech. Ministère l'Air, No. 345, 1958.
[28]J. C. André and M. Lesieur, "Influence of helicity on high Reynolds number isotropic turbulence," J. Fluid Mech. **81**, 187 (1977).
[29]J. R. Herring, "Approach of axisymmetric turbulence to isotropy," Phys. Fluids, **17**, 859 (1974).
[30]C. Garrett and W. Munk, "Internal waves in the ocean," Annu. Rev. Fluid Mech. **11**, 339 (1979).
[31]L. vanHaren, C. Staquet, and C. Cambon, "The decay of stratified turbulence: a numerical study," 8th Symposium on Turbulent Shear Flows, Munich, 7–9 September 1991.
[32]C. Teissèdre and K. Dang," Anisotropic behaviour of rotating homogeneous turbulence by numerical simulation," *Proceedings of the 19th AIAA Fluid Dynamics, Plasma Dynamics and Lasers Conference*, Honolulu, 1987 (AIAA, Washington, DC, 1987).
[33]C. Cambon, J. P. Benoit, L. Shao, and L. Jacquin, "Stability analysis and large eddy simulation of rotating turbulence with organized eddies," submitted to J. Fluid Mech.
[34]J. Chasnov (private communication).